Dynamic Simulation Model for an Autonomous Sailboat

Moritz C. Buehler Carsten Heinz Simon Kohaut

Sailing Team Darmstadt e.V.
{moritz.buehler, carsten.heinz, simon.kohaut}@sailingteam.tu-darmstadt.de

Abstract

Sailing without any human intervention generates a great fascination, since it is challenging while enabling many opportunities. Moving without external energy supply, possibly transporting goods, collecting plastic waste or recording scientific measurement data, new attractive scenarios become possible. As first milestone, we aim to send a robotic sailboat across the Atlantic ocean, coping with bad weather including storms, other vessels or floating waste.

For testing, designing control, sophisticated route planning, and managing algorithms, we are interested in differential equations for a simulation model. Therefore, we theoretically derive relations, describing the sailboat motion as those of a rigid body having six degrees of freedom (6 DOF). This allows us to reproduce significant nonlinear effects like the ones created by flow separation, speed dependence of the dynamics and oscillations by waves, while maintaining a comprehensible structure of the external forces of the sailboat. In contrast to standard velocity prediction programs (VPP), we are interested in the actual dynamical behavior, the effect of sail angles, rudder and waves while the precise prediction of the actual reachable velocities are of minor interest.

The dynamic model can serve for controller design and for the generation of test data. Additionally, it is used to feed a hardware model of our boat, providing an intuitive way of demonstrating the boat movements.

1 Introduction

For large parts of the oceans, accurate measurements of the environment are missing. More detailed data would benefit climate research and environment monitoring. A way to perform the ocean sensing is the usage of autonomous sailing boats. This reduces the cost of the required hardware from a big research vessel to a small boat and eliminates personnel costs as there is no crew on the ship. Further use cases are the collection of trash and cheap, energy efficient transportation of goods.

These long term missions through rough weather conditions require a high confidence in the hardware of the boat and in the algorithms. Therefore, a way to test the implemented controller is required. In this paper, we present a simulator to provide a basis for testing our developed algorithms and systems of an autonomous sailboat. This allows a short development cycle with fast feedback without the need to use a real boat. The

Accepted Publication to the International Robotic Sailing Conference 2018, Southampton, United Kingdom, 31-08-2018

focus is on a six degrees of freedom (6 DOF) model for a sailing boat. It is used for simulating the dynamic boat movement. Further it is important for controller design and a test pattern generator for the whole software architecture as well as for visualization purposes.

1.1 Related work

For modeling the dynamics of motorized vessels there is rich literature, e.g. (Fossen, 2005), however for wind propulsion, special effects have to be considered. The specifics of sailing are treated in models for yachts (Philpott et al., 1993) in the development of Velocity Prediction Programs (VPP). However, they aim to optimize the race performance and therefore focus on the achievable speed, while we are interested in the dynamic motion effects. Dynamic models for sailing vessels are derived in (Saoud et al., 2013), (Alves, 2010), (Masuyama and Fukasawa, 2011) and (Roncin and Kobus, 2004). However, (Masuyama and Fukasawa, 2011) concentrates on tacking, (Saoud et al., 2013) and (Alves, 2010) reduce the model to 3 DOF, neglecting the influence of roll and waves. (Roncin and Kobus, 2004) relies on the identification of a larger set of parameters based on experiments for which we would need a setup respectively CFD model. In contrast, we outline a 6 DOF model including wave effects while transparently formulating the acting forces using fewer parameters to obtain a rich but comprehensible simulation setting.

1.2 Assumptions

For our model, we take several assumptions. First, we neglect the change of the wind over the height and assume a constant wind speed as well as angle over the whole sail. A similar assumption is made for the lateral parts and the water speed. Also the interference between both sails is neglected. Each sail will change the wind locally which will have effects on the other sails. Instead, lift and drag coefficients of the sails are approximated by the results of thin airfoil theory, which additionally neglects the shape change of the sail. The flow separation is estimated in a simple model interpolating between unseparated and fully separated flow. For the waves, it is assumed, that the wave length is large compared to the ship length.

2 Mathematical model of the boat movement

To simulate the movement of the sailboat, we need a model in the form of differential equations, describing the temporal relations of external forces acting on the sailboat through dynamic and kinematic relations. For our use case, we are interested in a rich but comprehensible model, covering important effects of the sailboat's motion.

We model the dynamics and kinematics for a 6 DOF boat model, that depend on the geometries and inertia. A sailboat operates at the boundary between two media, water and air and uses speed differences to move forward. As important forces, we derive equations for the following components:

- sail, keel and rudder force
- buoyancy forces including effects from ocean waves
- wave resistance
- damping forces

2.1 Dynamics and kinematics

The dynamics describe how the forces acts on the boat speeds and turn rates due to the boat inertia. It is wise to derive the relations of forces and dynamics in different reference frames, that are connected through kinematic relations, see also Figure 1.

We describe the position x_g, y_g, z_g and heading ψ of the boat in our globally fixed or navigational frame, with $z = 0$ at the undisturbed water surface.

At the center of gravity of the boat, we locate the second, the heading frame, also parallel to the water surface with x axis in heading direction. The transformation from the global frame consists of the translation of position (x_g, y_g, z_g) and rotation according to heading ψ. In this heading frame, we formulate the buoyancy F_{hs}, the translation dynamics (change of speeds v_x, v_y, v_z) and the wave resistance F_{wr}. The basis vectors in the heading frame are denoted by $\{\mathbf{e}_x, \mathbf{e}_y, \mathbf{e}_z\}$.

The third frame is the body frame, fixed to the boat main axes. Here, it is intuitive to describe the rotational dynamics, sail, rudder and keel forces. The transformation from the heading frame is achieved by rotating due

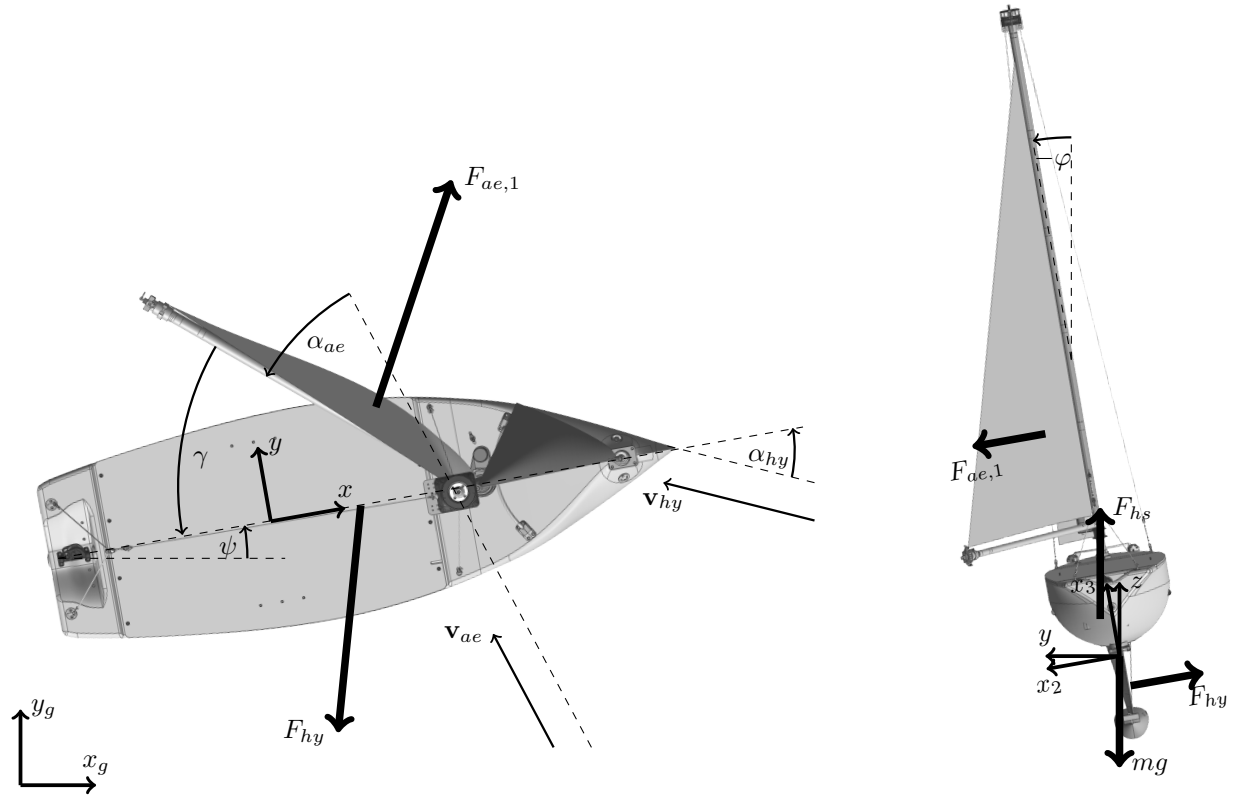

(a) (b)

Figure 1: Top view (a) and rear view (b): Forces of sail(s) F_{ae}, keel F_{hy} and buoyancy F_{hs}. Position (x_g, y_g, z) and heading ψ is measured in a global frame, buoyancy and lateral dynamics in a frame centered at the ship but oriented to the water surface, and the angular dynamics in a ship oriented coordinate frame. The aerodynamic angle of attack α_{ae} results from sail angle γ and apparent wind direction $\beta_{WA} = \gamma + \alpha_{ae}$, hydrodynamic α_{hy} from the leeway drift and water stream.

to roll angle φ, while the pitch angle θ is often negligible small. The basis vectors of this frame, we denote as $\{\mathbf{e}_1, \mathbf{e}_2, \mathbf{e}_3\}$.

Altogether, we have 12 states, the translations x_g, y_g, z_g, heading ψ, roll φ and pitch θ and the change rates in positions v_x, v_y, v_z and angles p, q, r, where $\mathbf{v} = v_x\mathbf{e}_x + v_y\mathbf{e}_y + v_z\mathbf{e}_z$ is the speed at center of gravity and $\Omega = p\mathbf{e}_1 + q\mathbf{e}_2 + r\mathbf{e}_3$ the angular velocity.

From the kinematics, we obtain the first part of differential equations, the position (ground based) changes according to heading and speeds,

$$\frac{d}{dt}\begin{pmatrix} x_g \\ y_g \\ z \end{pmatrix} = \begin{pmatrix} v_x\cos(\psi) - v_y\sin(\psi) \\ v_x\sin(\psi) + v_y\cos(\psi) \\ v_z \end{pmatrix}. \tag{1}$$

Similar holds for the angles, where it is used, that the pitch angle is small.

$$\frac{d}{dt}\begin{pmatrix} \varphi \\ \theta \\ \psi \end{pmatrix} \approx \begin{pmatrix} p \\ \cos(\varphi)q - \sin(\varphi)r \\ \cos(\varphi)r + \sin(\varphi)q \end{pmatrix} \tag{2}$$

The speed and angular rates change due to forces and moments according to the dynamic equations. The boat speed change due to overall applied forces $\mathbf{F}$ and boat mass m,

$$m\frac{d}{dt}\mathbf{v} = \mathbf{F}. \tag{3}$$

For the left side we need to respect the angular velocity of the heading frame, the change of heading, $m\frac{d}{dt}\mathbf{v} = m((\dot{v}_x - \dot{\psi}v_y)\mathbf{e}_x + (\dot{v}_y + \dot{\psi}v_x)\mathbf{e_y} + \dot{v}_z\mathbf{e}_z)$.

When the boat accelerates, surrounding water is accelerated, resulting in a transient hydrodynamic force that is usually modeled as an added mass. Additionally, this effect introduces cross terms, coupling roll and sway. We plan to include added masses soon in our description, since they have an important influence, especially for roll motion (Korotkin, 2009). Therefore, (3) and (4) have to be slightly adapted to include the coupling of inertia.

For the angular velocities, we have the relation of the angular momentum $\Theta\mathbf{\Omega}$ and overall torque $\mathbf{T}$,

$$\frac{d}{dt}(\Theta\mathbf{\Omega}) = \mathbf{T} = \sum_i \mathbf{r}_i \times \mathbf{F}_i, \tag{4}$$

where Θ is the angular inertia, $\mathbf{\Omega}$ the angular rate vector and $\mathbf{r}_i$ the vector from center of gravity to the ith force point of application. Due to approximate symmetries of the boat, the principal inertia axes do coincide with the boat main axes, leading to a diagonal inertia $\mathbf{\Theta}$ (apart from added masses). For the derivative, it is important to respect, that the ship itself is moving and the ship based coordinate frame itself has to be differentiated, $\frac{d}{dt}(\Theta\mathbf{\Omega}) = \dot{p}\Theta_1\mathbf{e}_1 + \dot{q}\Theta_2\mathbf{e}_2 + \dot{r}\Theta_3\mathbf{e}_3 + \mathbf{\Omega} \times \Theta\mathbf{\Omega}$. The formulation in ship based coordinates is however necessary to avoid a full and time dependent inertia matrix.

In the following we derive equations for the force components describing the motion of the sailboat, needed for equations (3) and (4).

For the aero and hydrodynamics, we have to differ apparent wind (stream) and the true wind (stream). The true wind is the wind referred to the ground, that is equal for all vessels at a given position. For the hydro- and aerodynamic forces, the relative flow is relevant, meaning that the ship speed has to be subtracted from the absolute. Hence the apparent or relative wind (and water flow) is calculated as the vectorial sum of the true wind (water stream) and the negative boat velocity. With raising boat velocity, the apparent wind changes its directions towards coming from ahead with varying strength. Additionally, the rotation of the boat changes the relative flow on the foils. Therefore, we chose the point of load $\mathbf{r}_{foil}$ of the foil and assume constant flow speed over the whole foil (which seems to be fine for not too large rotation rate). The relative velocity is calculated as $\mathbf{v}_{rel} = \mathbf{v}_{flow} - \mathbf{v} - \Omega \times \mathbf{r}_{foil}$. For the rudder this might be problematic due to the nearby keel but this remains for further refinement.

2.2 Sails and lateral foils

A main impact results from the sails and lateral plans, keel and rudder. Both, we model analog as ideal foils in a fluid stream. We calculate the resulting fluid forces based on results from theoretical aerodynamics, providing equations for lift and drag forces and the points of attack.

In difference to a hard foil where the actual shape is fixed, the shape of a sail varies according to load and design. However, we want to stay at a simple description combined with fast computation and neglect these effects.

2.2.1 Lift and drag

Lateral foils and sails are placed in a fluid stream that reaches them under a specific angle of attack α. For the keel, this is the relative angle of the water flow. For the sails, the apparent wind angle is referred to the sail angle γ (see Figure 1).

For the forces, we use the results from theoretical aerodynamics of thin foils leading to the relation for the lift coefficient as

$$c_L = c_{L,0} + c_{L,\alpha}\alpha, \tag{5}$$

where $c_{L,0}$ is the lift coefficient at zero angle of attack that is zero for a symmetric foil, and for thin foils a theoretic value of the slope coefficient of $c_{L,\alpha} = 2\pi$ is known (while neglecting the foil shape) (Spurk and Aksel, 2010).

The drag force of a foil consists of different components: Friction at the surface, induced drag due to finite foil height and pressure loss when it comes to flow separation that we treat later. At small angles of attack, the drag coefficient is

$$c_D = c_f + c_{D,i}. \tag{6}$$

The induced drag depends quadratically on the lift coefficient $c_{D,i} = c_L^2/(\pi\Lambda)$ with the geometric foil stretching Λ, height h and area A. The theoretical friction coefficient of a plate in laminar flow is $c_f = 2.66/\sqrt{Re_l}$ (Spurk and Aksel, 2010), where $Re_l = \frac{vl}{\nu}$ is the Reynolds number with length l of the plate in direction of the flow and ν is the kinematic fluid viscosity.

With drag and lift coefficients we can calculate the forces by multiplying the dynamic pressure $q = 0.5\rho v_{rel}^2$ and the area A,

$$\mathbf{F}_{flow} = qA\left[(\sin(\beta_{WA})c_L - \cos(\beta_{WA})c_D)\mathbf{e}_1 - (\sin(\beta_{WA})c_D + \cos(\beta_{WA})c_L)\mathbf{e}_2\right], \tag{7}$$

that is transformed to the ship based frame according to the relative flow angle β_{WA}.

The point where the aerodynamic force acts, is for the flat symmetric wing at one forth length, but varies until one third for asymmetric shapes where the location depends on the angle of attack (Spurk and Aksel, 2010).

2.2.2 Flow separation

At larger angles of attack (e.g. sailing in front of the wind for the sail, departing from low speeds for the keel), the flow separates from the foil, the lift reduces and the drag by the pressure loss gains significant influence. In the extreme case of an angle of attack of 90 degrees, there is no lift (due to symmetries), while the drag coefficient is slightly above $c_D \approx 1$ and the point of attack is the center of the foil. At smaller angles, we model the drag coefficient as $c_D = \sin(\alpha)^2$ representing the dynamic pressure of the flow perpendicular to the foil. For most foil shapes, flow separation leads to stall angles, the angle where c_L is maximal, between 15 and 25 degree. We interpolate between not separated case and flow separation heuristically according to a separation factor $s = 1 - \exp\left[-(\alpha/\alpha_{sep})^2\right]$ and use a characteristic angle $\alpha_{sep} = 25°$, resulting in a stall angle of 15°.

2.3 Wave resistance

The velocity of a displacement vessel is limited by the wave resistance at maximum hull speed. This resistance results from the waves generated by the ship movement. At about a Froude number of $Fr = v/\sqrt{gl_{wl}} = 0.4$, the wave resistance reaches a local maximum that cannot be exceeded by our keel boat.

The maximum hull speed depends on the square root of the waterline length l_{wl} of the ship $v_{hull} = 0.4\sqrt{gl_{wl}}$, resulting to a maximum speed for a 4 m water line length of about 2.5 m/s.

We approximate the wave drag by a 6th order polynomial introducing it as speed limiting factor, neglecting the hull shape dependent interference effects and model the wave resistance according to

$$\mathbf{F}_{wr} = -\operatorname{sign}(v_x)c_{wr}q_{hy}A_{LK}\left(\frac{v_{hy}}{v_{hull}}\right)^4\mathbf{e}_1, \tag{8}$$

with lateral area A_{LK} and a wave resistance weight parameter c_{wr}.

2.4 Hydrostatic buoyancy and wave influence

The hydrostatic force is central for the boat to float on the water and the moment stabilizes roll and pitch angles.

The hydrostatic bouyancy respectively Froude-Krylov force (Fossen, 2005) is the integrated water pressure over the hull, also described as the weight of displaced water. For the calculation of the pressure, the virtual water surface without the vessel has to be used. In calm water and zero speed, the hydrostatic force acts vertically (along z_g), compensating the vessels weight at the stationary point of floating. With some elevation of the ship z_g or similarly an actual wave elevation η, the hydrostatic force F_{hs} is calculated as

$$F_{hs} \approx mg + \rho_{hy}gA_W(\eta - z_g), \tag{9}$$

with gravity acceleration g, water density ρ_{hy} and the water plane area at equilibrium A_W. The integration of the waterline surface changes is neglected leading to the above linear relation.

The point where the force acts depends on the height difference of the buoyancy point above the center of gravity $h_{hs,0}$ and the second moments of water plane area $I_{L/T}$.

For the side shift, we get

$$\mathbf{r}_{hs} \approx -\left(\frac{\rho_{hy}}{m}I_L + h_{hs,0}\right)\sin(\varphi_{eff})\mathbf{e}_y + \left(\frac{\rho_{hy}}{m}I_T + h_{hs,0}\right)\sin(\theta_{eff})\mathbf{e}_x, \tag{10}$$

again neglecting the change of the water plane due to roll and heave. The first part of each component respects the stabilizing influence of the hull shape of the ship, the second the influence of the static deviation from the center of gravity. The second moment of water plane area I_T for the pitch movement is at a larger order than I_L for the roll movement due to the lengthiness of common boat shapes. Therefore, pitch angles stay small especially in the absence of waves.

The effective hydrostatic roll angle has to be referred to the water surface including waves. With the wave elevation field $\eta(\mathbf{x}, t)$ it becomes $\varphi_{eff} = \varphi - \arctan\left(\frac{\partial \eta}{\partial y}\right)$ and $\theta_{eff} = \theta + \arctan\left(\frac{\partial \eta}{\partial x}\right)$, where it is assumed, that the wave length is large compared to the ship length (4 m), which should be the case for offshore ocean waves with significant amplitudes.

The buoyancy force changes the direction according to the water surface, and partially acts in horizontal directions, again linearized to $\mathbf{F}_{hs} = F_{hs}\mathbf{e_z} - F_{hs}\frac{\partial \eta}{\partial x}\mathbf{e_x} - F_{hs}\frac{\partial \eta}{\partial y}\mathbf{e_y}$.

2.5 Damping

Lastly, we model linear constant damping of the boat, though the addition of a quadratic term will be more appropriate. The used damping force and moment are $\begin{pmatrix}\mathbf{F}_D & \mathbf{T}_D\end{pmatrix} = -\mathbf{d}\begin{pmatrix}\mathbf{v} & \mathbf{\Omega}\end{pmatrix}$,where we use decoupled, rough estimates for the damping parameters $\mathbf{d}$.

2.6 Inputs

For a simulation, we have to specify all external variables like wind and waves as well as control variables, rudder and sail angles. The first are part of the simulation environment, while the latter have to be chosen by a boat controller.

For the rudder, a limitation ($\pm 35°$) is used. For the choice of the rudder angle, the flow separation at high angles of attack of the rudder has to be avoided or respected during controller design. For the sails, the possible angle is geometrically restricted by shrouds ($\pm 90°$). A stronger constraint is imposed by the limited rate of change for which we introduce a first order model in the next part. Additionally, for practical reasons of energy management, the sail angle should not be changed too often. An adaption seems to be necessary mainly at maneuvers and changes in heading and wind. In contrast, the rudder is important to control the heading and reducing the impact of disturbances like waves or wind gusts. We choose a sample time of 100 ms, but its value may be adapted according to energy resources and control requirements.

2.6.1 Limited actuator speeds

It is not possible to set sail and rudder angles immediately, instead changing them requires time and energy. The actuators have to change the rope length (sail) or the rudder position. To respect this in a simple way, we chose a first order linear behavior determined by some time constant τ describing the typical time for the rudder respectively sail to be set. This temporal behavior results from the actuator position controllers. Additionally, the absolute change rate may be limited due to a maximum actuator speed.

The time constant of the rudder is assumed to be short (0.1 s), while for the sail we expect a larger time constant due to hardware design (e.g. 3 s). For the sails, the actuation by ropes implies another effect: Its angle can change very fast during jibing or tacking. It is rather the maximum absolute angle that is chosen by the controller setting the length of the rope. The side respectively sign of the sail angle is chosen by the relative wind.

2.7 Implementation and numeric integration of the differential equations

For the simulation, the differential equations of the dynamics model (1)-(4) have to be integrated departing from the initial state values $\mathbf{x_0}$. Therefore we use the Dormand Prince method, a standard Runge-Kutta method with adaptive step size. For a simulation time of 120 seconds, 2 seconds computation time is needed on 2 GHz single CPU computation.

The implementation of our simulation setup is available at `https://github.com/simko96/stda-sailboat-simulator`.

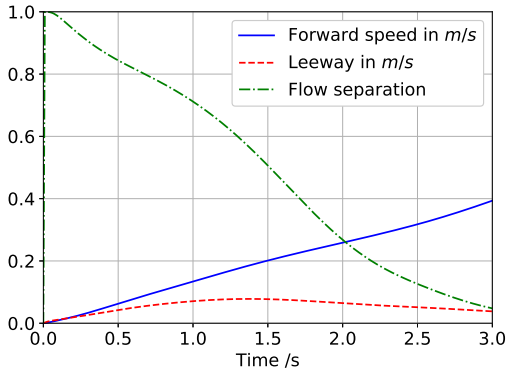

Figure 2: Boat accelerating from zero speed. Forward speed v_x and leeway v_y are both rising, until the overall speed augments and the keel compensates the side force. The high initial leeway drift angle leads to flow separation.

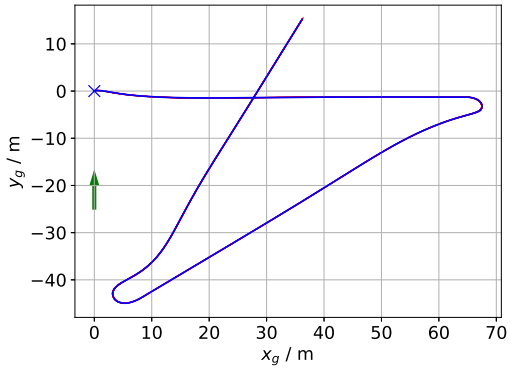

Figure 3: Simulated ship trajectory: Gaining speed tacking and jibing; boat starts at blue cross, wind direction is marked by the green arrow.

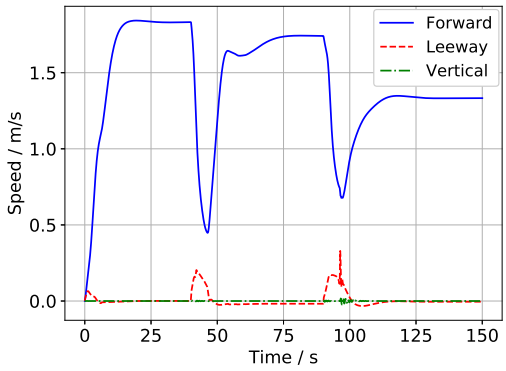

Figure 4: Speed of the boat in the different directions: Horizontal speed is almost decoupled, hence close to zero in the absence of waves.

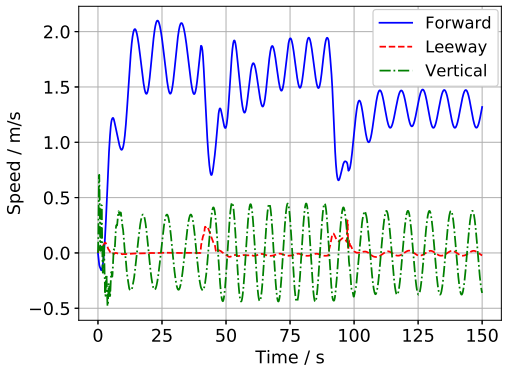

Figure 5: Same simulation scenario but with waves: Ship speeds for a wave field with 1 m wave height at a wave length of 100 m, arriving from right.

3 Simulation

The simulator should be able to reproduce main effects of the sailboat dynamics to deliver useful data for testing software components like controllers or path planning. One interesting situation is the departure from zero speed, where the effects of rudder and keel differ from normal operation (here the inertia dominates). Other interesting situations include state changes during maneuver execution and the influence of bigger waves. The simulation serves as data generation to test our modules like heading controller, path planning or filter algorithms. However, so far we do not have empirical data to validate its performance. Instead we qualitatively examine for plausibility.

3.1 Scenario: gaining speed, tacking and jibing

Our scenario consists of the boat accelerating at departure from zero speed, while the wind comes from south with 5m/s (right angle to initial heading), followed by tack and jibe maneuvers (Figure 3). Therefore, we use a feedback control for the heading through the rudder, that is derived from a simplified nonlinear dynamics model for the yaw motion, and a feed forward control of the sails.

The first part of the scenario is to gain speed (Figure 2). At departure, there is no water flow which leads to a high initial leeway (acceleration according to the sail force), and the starting flow separates. While the boat speeds up, the keel force raises until it compensates for the side force of the sails.

At tacking, the speed reduces due to the missing propulsion when crossing the wind. Afterwards, the boat speeds up at the new heading. For jibing, the speed decrease is less pronounced (Figure 4). During both

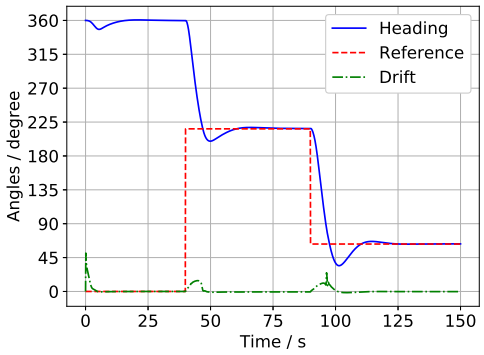

Figure 6: Plot of the controlled heading angle, its reference and the leeway drift angle compensated by the controller.

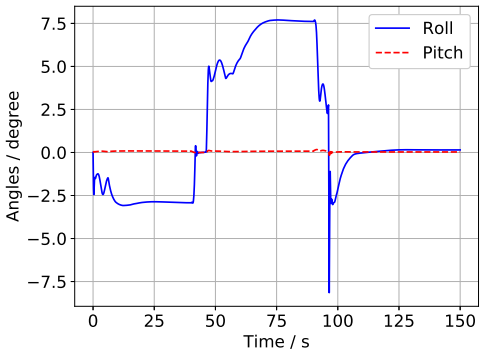

Figure 7: Corresponding angles in roll and pitch, due to the high longitudinal stability (geometric inertia), the pitch angle remains small.

maneuvers, the roll angle changes the sign. The pitch angle remains negligible during the scenario (Figure 7) and becomes larger but still small when introducing waves (not shown). The heading (controlled by use of the rudder) is shown in Figure 6.

With waves of 1 m height coming from east ($-x_g$-direction), the base trajectory looks similar. Oscillations induced by the waves are superposed on all states, exemplary shown for the speeds in Figure 5.

3.2 Visualization by hardware model

Another application is the data generation for our movable hardware model of the boat shape that serves for demonstration and visualization issues (Figure 8). It is eligible when presenting our project, e.g. at fairs, and useful to test interfaces between the different components, software, electronics and actuators.

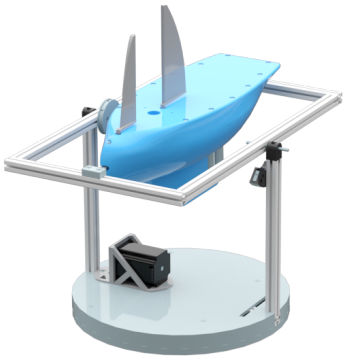

Figure 8: Demonstration model of a sailing boat.

4 Conclusion

In this paper, we derived the differential equations describing the dynamics of a sailboat, by considering the forces generated by both fluid flows, wind and the relative water stream.

This model is used, to simulate the sailboats motion, particularly for maneuvers like tacking or jibing. The simulation results seem plausible and well suitable for our demonstration model. Further, it is useful for testing our control and path planning algorithm.

However, we still need to record real data, to identify parameters like damping and compare and evaluate the simulation quality.

References

Alves, C. (2010). Sailbot: Autonomous marine robot of eolic propulsion. Master's thesis, Instituto Superior Tecnico, Universidade Tecnica de Lisboa.

Fossen, T. (2005). A nonlinear unified state-space model for ship maneuvering and control in a seaway. *Journal of Bifurcation and Chaos*, 15:2717–2746.

Korotkin, A. (2009). *Added Masses of Ship Structures*. Springer.

Masuyama, Y. and Fukasawa, T. (2011). Tacking simulation of sailing yachts with new model of aerodynamic force variation during tacking maneuver. *Journal of Sailboat Technology*, 119.

Philpott, A. B., Sullivan, R. M., and Jackson, P. S. (1993). Yacht velocity prediction using mathematical programming. *European Journal of Operational Research*, 67:13 – 24.

Roncin, K. and Kobus, J. (2004). Dynamic simulation of two sailing boats in match racing. *Sports Engineering*, 7:139–152.

Saoud, H., Hua, M., Plumet, F., and Amar, F. (2013). Modeling and control design of a robotic sailboat. *Robotic Sailing*.

Spurk, J. and Aksel, N. (2010). *Stroemungslehre*. Springer.